

# FEM Numerical Simulation and Experimental Investigation on End-Forming of Thin-Walled Tubes Using a Die

Lirio Schaeffer, Alberto M. G. Brito

Metal Work Laboratory, Universidade Federal do Rio Grande do Sul, Porto Alegre, Brazil, brito@ufrgs.br

Thin-walled tubes are applied in several industrial areas, as heat exchangers, shock absorbers, preforms to other metal forming processes, etc. In this study an experimental and theoretical investigation is performed involving tube end expansion, reduction and inversion processes using a die. The parameters that govern each process are investigated. A brief description of each process and a summary of the state of art are presented. The material employed in the experimental tests is an AISI 1010 carbon steel and all the work is carried out at room temperature. The theoretical investigation is done using FEM software QFORM 3D, version 4.1.5. In order to feed the software with realistic data stress-strain curves for the material were obtained by means of compression tests and the tribological conditions at the contact interface between the tube and the tools was estimated by means of ring compression method. The investigation on the tube end-forming processes focused mainly on understanding modes of deformation and on establishing formability limits for each of them. The results show that processes for end-forming of thin-walled tubes are successful only within a compact range of process parameters.

**Keywords:** Finite element method; Computer simulation; Thin-walled tubes; End-forming processes; QForm 3D.

## Introduction

Thin-walled tubes are applied in several industrial areas as heat exchangers, shock and energy absorbers, setting systems, preforms for other metal working processes, etc. Usually the production of these parts involves the execution of finishing or setting operations in the tube extremity [1-4]. These operations can be divided into four types that can be combined to generate a great number of geometric forms [5]. **Figure 1** shows the four basic modes of operation: expansion, reduction, external inversion, and internal inversion.

During end-forming tube operations the material is subjected to strain hardening. This phenomenon, the geometric characteristics and the frictional conditions define the feasibility of the process and the final mechanical properties of the tubular part.

Plastic deformation is the result of three different mechanisms: bending and/or 'unbending', stretching or compression along the circumferential direction,  $\theta$ , and friction.

In expansion and reduction the main geometric parameters are the angle,  $\alpha$ , of the punch or die (see Figures 1a and 1b) and the deformation degree along the diameter. In an expansion process the first contact between the tube and the punch is characterized only by the slide between the surfaces of the tube and the punch. The plastic deformation begins at point B, where the tube starts bending until point C. Between points C and D tube stretching occurs along the circumferential direction. The 'unbending' occurs between points D and E where the tube no longer has contact with the punch. Between points E and F there is a deformation free region where the behavior of the tube is close to that of a rigid body. The main influence of friction occurs between points B and D. The reduction process can be described as having a similar form. A difference is that between points C and D the tube is compressed in the circumferential direction.

The external inversion process occurs as shown in Figure 1c. Bending occurs at point B, where the tube has the first

contact with the die and at point D where the 'unbending' takes place. Stretching occurs along the circumferential direction while the tube is deformed against the die radius, from point B until point D. The friction exerts influence from point B to point C where there is contact between the tube and the tool. The internal inversion process (Figure 1d) runs in analogous form to the previous one, bending at point B and 'unbending' at point D. However, in contrast to the previous case, the tube is compressed between points B and D. The influence of the friction occurs in the interface tube/die between points B and C.

Several papers [1-5, 10-12] on the end-forming process of thin-walled tubes carried out with aluminium alloys demonstrate the existence of different modes of tube deformation. Besides the desired mode of deformation in each process, other modes can occur and make the process impracticable.

In the expansion process formability is limited by the occurrence of local buckling when high ratios of  $r_p/r_0$  and small expansion lengths are used. On the other hand, if large expansion lengths are used, the limitation of the process is due to the occurrence of ductile fracture in the highly stretched regions in the circumferential direction. In the reduction process the occurrence of local buckling seems to be the factor that limits the feasibility of the process to small and to large reduction lengths.

In the external inversion process the tubes suffer local buckling when a small die radius is used. An excessively large die radius fracture is observed due to the high tensile stresses developed in the circumferential direction. In internal inversion only local buckling is observed if a successful process is not achieved.

The main objective of this paper is to review and extend knowledge of end-forming processes of thin-walled tubes by means of a theoretical and experimental investigation. Emphasis is focused on understanding the parameters that govern each process seen in **Figure 1**.

The processes are investigated through numerical simulation using the finite elements method with commercial soft-

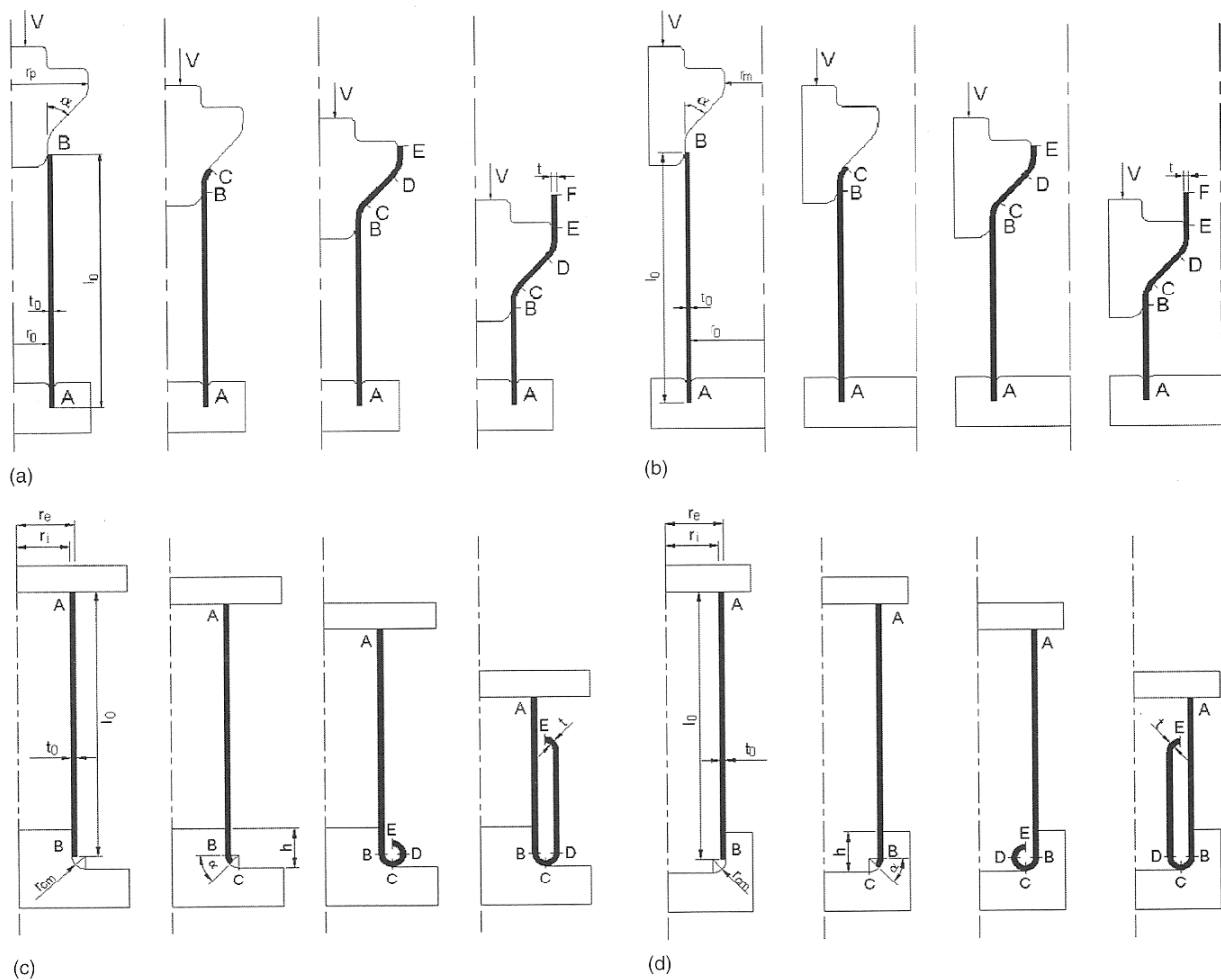


**Figure 1.** Four end-forming tubes processes: (a) expansion; (b) reduction; (c) external inversion; (d) internal inversion.

ware QFORM 3D, version 4.1.5. The processes are carried out at room temperature. The experimental work is performed for the purpose of supporting and validating the numerical simulations carried out.

## Literature Review

**Expansion and reduction.** Literature on end-forming tube processes is relatively rare. The first work found on expansion and reduction processes was published by Avitzur [6] in 1965. In 1996, Sadok et al. [7] used the finite elements FORGE2 software to calculate the force and strain distribution in an expansion process. In 1997, Um and Lec [8] presented an upper bound solution to tube drawing processes with a fixed plug and considered that the solution for the reduction process can be obtained with friction between the tube and the plug becoming equal to null. In 1998, Ruminski et al. [9] used FORGE2 software to study the effect of convex and concave dies in a reduction process. In 2006 Alves et al. [10, 11] and Almeida et al. [12] carried out theoretical and experimental investigations on the expansion and

reduction processes of aluminium alloys with IFORM 2D/3D software.

**Inversion processes.** In 1966, Guist and Marble [13] carried out the first related experiences with the free external inversion of tubes. A few years later, in 1972, Al-Hassani, Johnsons and Lowe [14] developed detailed investigations on the external inversion of tubes using a die. In that work a rigid plastic model was assigned to the material and a null value to the friction. In 1976, Al-Qureshi and Morais [15] investigated experimentally and analytically the external inversion of copper and brass 70/30 tubes. They developed an analytical treatment similar to that presented by Al-Hassani [14] but with the inclusion of the friction effect in the contact area between the tube and the die. The following year Al-Qureshi and Morais [16] extended this analysis to the internal inversion process. The internal inversion of tubes was studied in 1983 by Kinkead [17] and included strain hardening of the material, friction in the tube/die interface and variation of tube wall thickness during the process. Between 1986 and 1999, Reddy, Reid, Harrigan and Peng studied the external [18-20] and internal [21, 22] inversion

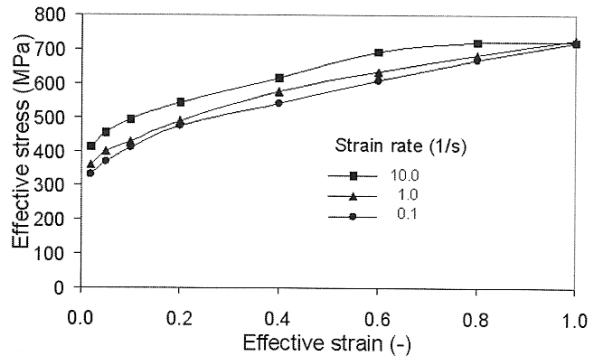


**Figure 2.** Flow curves for AISI 1010 carbon steel at room temperature.

of metallic tubes using the ABACUS software. In 1992, Yang and Zhaorong [23] presented a model to determine the die radius for which the tube can be inverted without the occurrence of plastic instability or rupture. The first intensive study of tube inversion using the finite elements method seems to have been developed in 2001 by Yang et al. [24, 25]. In 2003, Rosa et al. [1, 2] presented the results of extensive study on the external inversion of thin-walled tubes in a die, guided towards understanding deformation modes that are associated with the definition of formability limits. In 2004, Rosa et al. [3] transposed the methodology used in the work with external inversion [1, 2] to investigate the parameters that define the internal inversion process. In the same year Brito et al.[4] carried out studies on the internal inversion process emphasizing the influence of friction.

### Theoretical Background

QFORM-3D code is based on the flow formulation where independent variables are velocity vector and mean stress [26]. This kind of formulation means that the follow variational equation must be solved:

$$\int_v \bar{\sigma} \delta \bar{\epsilon} dV + \int_v p \delta \dot{\epsilon}_v dV + \int_v \dot{\epsilon}_v \delta p - \int_s F_i \delta v_i dS = 0 \tag{1}$$

where  $\bar{\sigma}$ ,  $\dot{\epsilon}_v$ ,  $\dot{\epsilon}$  and  $\delta v_i$  are, respectively, the effective stress, the effective strain rate, the volumetric strain rate and an arbitrary variation of the velocity field,  $p$  is the pressure,  $F_i$  means the external stresses applied on the body surface and  $V$  and  $S$  are the volume and surface of the part. A rigid-visco-plastic model is used for the material that is considered incompressible, isotropic continua and elastic deformations are neglected. The effective stress is a function of effective strain, effective strain-rate and temperature. The friction model that describes the part/die surface contact was proposed by Levanov [27] and can be written as:

$$f_\tau = K_p \tau_{sk} [1 - \exp(-1, 25 f_v / \sigma_{sk})] \tag{2}$$

where  $f_\tau$  is friction stress at a given point of the slip surface,  $\sigma_{sk} = \sqrt{3} \tau_{sk}$  is resistance to deformation for a thin near-contact layer,  $f_v$  is normal stress and  $K_p$  is a constant

that depends on the state of the friction surfaces as roughness, adhesion properties and the presence of a lubricant film [27].

### Simulation Planning

The simulation work was planned based on the experience acquired in previous studies on end-forming processes of tubes carried out with aluminum alloys [1-5, 10-12].

The external and internal inversion processes were studied with tubes 100 mm long, walls 2 mm thick and external diameter 50.8 mm. The study was carried out to verify process feasibility as a function of the die radius,  $r_{cm}$  (Figure 1). Five different die fillet radii (2.54, 5.08, 7.62, 10.16 and 12.70 mm) were tested. Thus the ratios  $r_{cm}/r_e$  between the fillet radius of the die and the outer radius of the tube were 0.1, 0.2, 0.3, 0.4 and 0.5. In the case of the internal inversion an additional die radius equal to 4.5mm ( $r_{cm}/r_e=0.177$ ) was used.

In an expansion (or reduction) process the influence of expansion degree (or reduction degree) and of the punch (or die) angle on the process feasibility was studied. In both cases the angles were 15, 30 and 45°. In expansion deformations of 20, 40 and 60% were used, corresponding to an outer radius of 30.48, 45.56 and 40.64 mm to the tube. In reduction the deformations were equal to -20, -40 and -60%, corresponding to outer radii of 20.32, 15.24 and 10.16 mm. In these cases 200 mm-long tubes were used.

### Experimental Background

**Flow curves.** In the experimental tests AISI 1010 carbon steel was used. The stress-strain curve was obtained by means of compression tests in different strain rate conditions (0.1, 1.0 and 10.0 s<sup>-1</sup>) and at room temperature. The compression test samples were machined with a 10 mm diameter and 15 mm height from a 12.5 mm diameter cold drawn rod. **Figure 2** shows the curves obtained. The curves were loaded onto the software by means of a table.

**Friction factor.** Ring compression tests at room temperature were employed to estimate the tribological conditions at the tube/tools interface. Ring samples with a ratio of 6:3:2 were used. The tools for these tests were polished and MoS<sub>2</sub> was used for lubrication. Under these conditions the constant,  $K_p$  (equation 2) was determined by means of an inverse calibration technique using software QFORM and was found to be equal to 0.02. **Figure 3** shows the calibration curves which present the relative variation of the internal radius versus the relative variation of the height for constant values of  $K_p$ . In addition, some experimental points are presented.

**Expansion tube tests.** The experimental work on tube expansion confirmed the existence of three different modes of deformation. For large ratios  $r_p/r_0$  and small expansion lengths (high values of the angle) the process feasibility is limited by the occurrence of plastic instability. On the other hand, for large expansion lengths (small values of the angle) the limit of the process is the occurrence of ductile frac-

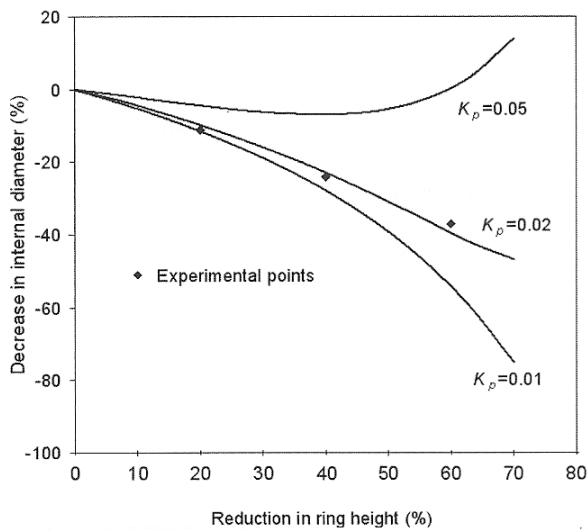


Figure 3. Calibration curves for constant values of the friction factor,  $K_p$ , and experimental values of the ring test.

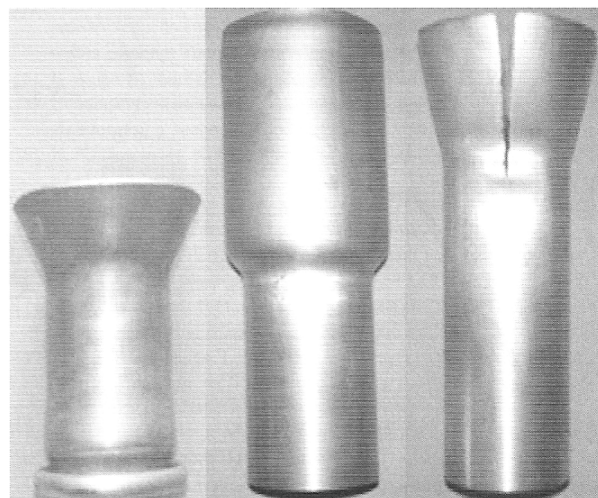


Figure 4. Three different modes of deformation observed in experimental work of the expansion process (from left to right: local buckling, expansion and fracture).

ture in the highly stretched regions in the circumferential direction. Figure 4 shows three of the tested samples, each one presenting a mode of deformation.

### Simulation Results and Discussion

**Expansion.** The simulations of the expansion process reproduced the experimental results and confirmed the existence of three modes of deformation: local buckling, expansion and fracture. Figure 5 shows force-displacement curves calculated for the three experimental cases in Figure 4. The figure also shows the geometries calculated using software QFORM 3D, which present excellent agreement with the experimental results.

**Reduction.** The simulation of the reduction process indicated the existence of two modes of deformation for the tubes: reduction or plastic instability. Among the cases analysed only those in which the deformation was 20% had resulted in successful processes. In the other cases local buckling occurred. Figure 6 shows the force-displacement curves of the cases with 20% and 40% deformations and die angle equal to 45°. In the case of the

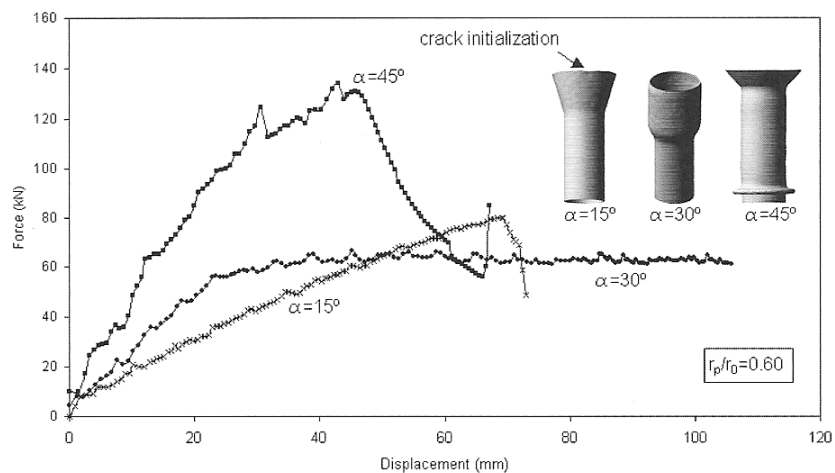


Figure 5. Force-displacement curves and final geometries calculated by software QFORM for the expansion process when the ratio  $r_p/r_0=0.6$  and  $\alpha$  equal to 15, 30 and 45°. The results show good agreement with the experimental cases in Figure 4.

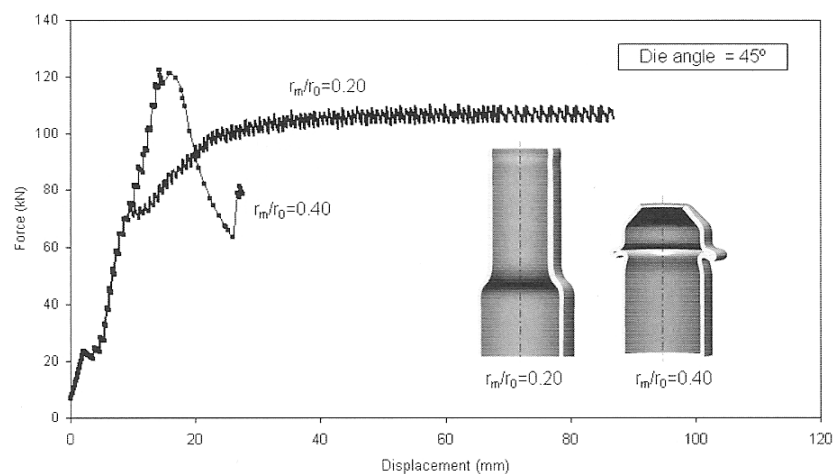
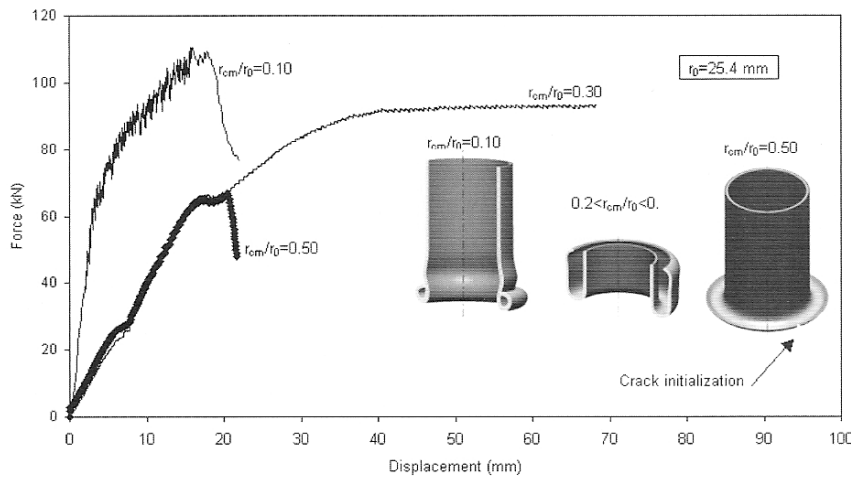
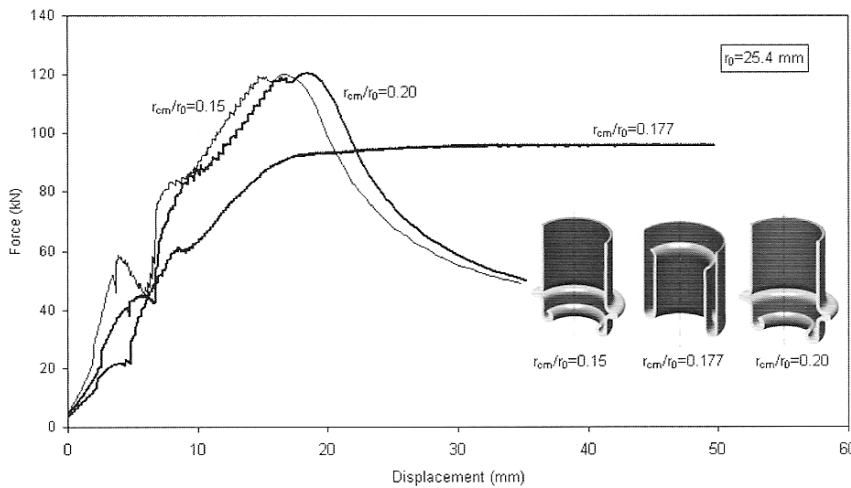


Figure 6. Force-displacement curves in the reduction process when  $r_m/r_0=-0.2$  and  $r_m/r_0=-0.4$  and the die angle is 45°.



**Figure 7.** Force-displacement curves and the final geometries calculated by the software for the three modes of deformation in the external inversion process when  $r_{cm}/r_e$  is equal to 0.10, 0.3 and 0.50.



**Figure 8.** Force-displacement curves and final geometries calculated by the software for three different cases in the internal inversion process. The process was only successful with a fillet die radius equal to 4.5 mm ( $r_{cm}/r_e = 0.117$ ).

successful process the force-displacement curve shows two distinct stages. In the first stage the curve grows until about 110 kN. Beyond this point the load stabilizes and the process becomes stationary. When local buckling occurs, two stages in the curve can also be observed. In the first, force grows approximately until 120 kN. At this point the critical instability load is reached, and force decreases while the material folds on itself. Process continuity leads to the occurrence of successive force peaks while new folds are formed. The instability load calculated by the software is compared with a value calculated by Timoshenko [28] tangent-modulus approach,

$$\sigma_{cr} = \frac{1}{\sqrt{3 \cdot (1 - \nu^2)}} E_t \frac{t_0}{r} \quad (3)$$

where  $\nu$  is the Poisson ratio and  $E_t$  is the tangent modulus of the material defined as the slope,  $d\sigma/d\varepsilon$ , of the flow stress curve in the plastic range at the current value of  $\sigma = P/A$ .

The discrepancy between the critical stress calculated by the software (391 MPa) and that calculated by the tangent-modulus method (350 MPa) is about 12 %.

**External inversion.** Similar to the expansion process, three modes of deformation are identified in the external inversion process: instability, inversion and rupture. Local buckling occurs when a small fillet radius is used in the die ( $r_{cm}$  in Figure 1). When a very large fillet radius is used in the die, the material fractures. The rupture is caused by the tensile stresses along the circumferential direction as well as by the wall thickness reduction when the inversion approaches 180°. **Figure 7** shows the force-displacement curves and the final geometries calculated by the software for the three modes of deformation. In the case where local buckling occurs, the curve grows until about 110 kN when the critical instability load is reached. Then the tube buckles and the force decreases. This mode of deformation occurs when the ratio between the fillet radius of the die and the outer radius of the tube ( $r_{cm}/r_e$ ) is 0.1. At the ratio  $r_{cm}/r_e = 0.5$  fracture was observed. In this case the force grows until about 70 kN and decreases quickly when the rupture starts. The process was successful

when ratios  $r_{cm}/r_e$  equal to 0.2, 0.3 and 0.4 were used. In these cases the force grows until the process becomes stationary.

**Internal inversion.** In the internal inversion process two modes of deformation were observed during the simulation with different parameters: inversion and instability. Fracture is not observed because in this process stresses in the circumferential direction are compressive. However, the range of ratio  $r_{cm}/r_e$  where the process is feasible seems to be smaller in the external inversion process. **Figure 8** shows the force-displacement curves and final geometries calculated by the software for three different cases. Only for a fillet die radius equal to 4.5 mm ( $r_{cm}/r_e = 0.117$ ) was the process successful. Out of the range  $0.1 \leq r_{cm}/r_e \leq 0.2$  local buckling was observed. In the successful case the force-displacement curve grows until about 95 kN and then a steady-state stage is reached. In the other cases the force grows until about 120.13 kN when  $r_{cm}/r_e = 0.1$  and until 124.38 kN

when  $r_{cm}/r_e = 0.2$ . When the critical instability load is reached, the tube buckles and the force decreases quickly.

## Conclusions

The manufacture of sound thin-walled tubular parts by expansion, reduction and external or internal inversion using a die seems to be limited to components with a compact geometrical features range. This work shows that the parameters that govern the processes are the ratio  $r_{cm}/r_e$  and the angle of the conical surface of the punch (in expansion) or die (in reduction). Probably, the ratio between the thickness of the tube wall and its initial radius also play an important role in the feasibility of the process. However, it is not verified in the cases analysed in this work. For the expansion process the simulation and the experimental work confirmed in the case of steel tubes that for large ratios of  $r_{cm}/r_e$  and small expansion lengths (high values of the punch angle), the occurrence of local buckling limits the formability. On the other hand, for large lengths of expansion (small values of the punch angle) the limitation is the occurrence of ductile fracture.

In the inversion processes the ratio  $r_{cm}/r_e$  between the fillet radius of the die and the outer radius of the tube seems to be the main parameter that governs the process. External inversion is limited by occurrence of buckling for small values of  $r_{cm}/r_e$  while large values of the ratio favour the onset of cracks along the circumference. In internal inversion the range of the ratio  $r_{cm}/r_e$  at which the process is successful seems to be much more restricted than in external inversion. In internal inversion the process is limited by the occurrence of plastic instability (buckling) at small and large values of the ratio  $r_{cm}/r_e$ .

(A2007068; accepted on 5 June 2007)

## References

- [1] P. A. R. Rosa, J. M. C. Rodrigues and P. A. F. Martins: International Journal of Machine Tools and Manufacture, 43 (2003), 787/796.
- [2] P. A. Rosa, R. M. O. Baptista, J. M. C. Rodrigues and P. A. F. Martins: International Journal of Plasticity, 20 (2004), 1931/1946.
- [3] P. A. Rosa, J. M. C. Rodrigues and P. A. F. Martins: International Journal of Machine Tools and Manufacture, 44 (2004), 775/784
- [4] A. M. G. Brito, P. A. R. Rosa, J. M. C. Rodrigues, L. Schaeffer and P. A. F. Martins: Forming of thin-walled tubes using a die: theoretical and experimental investigation, Proc. 59<sup>th</sup> ABMM International Congress, 2004, São Paulo, Brazil
- [5] A. M. G. Brito: Análise teórico-experimental dos processos de expansão, redução e inversão de extremidades de tubos de parede fina em matriz, Dr.Eng. Thesis, Porto Alegre, Brazil, 2006.
- [6] B. Avitzur: Journal of Engineering for Industry, 87 (1965), p. 71/79.
- [7] L. Sadok, L. Kusiak, M. Packo and M. Ruminski: Journal of Materials Processing Technology, 63 (1996), 161/166.
- [8] K. K. Um and D. N. Lec: Journal of Materials Processing Technology, 63 (1997), 43/48.
- [9] M. Ruminski, J. Kuksza, J. Kusiak and M. Packo: Journal of Materials Processing Technology, 80 (1998), 683-689.
- [10] M. L. Alves, B. P. P. Almeida, P. A. R. Rosa and P. A. F. Martins: Journal of Materials Processing Technology, 177 (2006), 183/187.
- [11] M. L. Alves, B. P. P. Gouveia, P. A. R. Rosa and P. A. F. Martins: Journal of Engineering Manufacture, 220 (2006), 823/835.
- [12] B. P. P. Almeida, M. L. Alves, P. A. R. Rosa, A. G. Brito and P. A. F. Martins: International Journal of Machine Tools and Manufacture, 46 (2006), 1643/1652
- [13] L. R. Guist and D. P. Marble: Prediction of the inversion load of a circular tube, NASA TND 3622, 1966.
- [14] S. T. Al-Hassani, W. Johnson, W. T. Lowe: Journal Mechanical Engineering Science, 14 (1972), 370/381.
- [15] H. A. Al-Qureshi, G. A. DeMoraes: Analytical investigation of thin-walled tube expansion by the inversion process, Design Engineering Conference & Show, Paper No. 76-DE-9, The American Society of Mechanical Engineers, Chicago, 1976.
- [16] H. A. Al-Qureshi, G. A. DeMoraes: Analysis of multi-inversion of tube ends, Design Engineering Conference & Show, Paper No. 77-DE-35, The American Society of Mechanical Engineers, Chicago, 1977.
- [17] A. N. Kinkead: The Journal of Strain Analysis for Engineering Design, 18 (1983), 177/188.
- [18] T. Y. Reddy and S. R. Reid: International Journal of Mechanical Sciences, 28 (1986), 111/131.
- [19] T. Y. Reddy: International Journal of Mechanical Sciences, 34 (1992), 761/768.
- [20] S. R. Reid: International Journal of Mechanical Sciences, 35 (1993), 1035/1052, 1993.
- [21] S. R. Reid and J. J. Harrigan: International Journal of Mechanical Sciences, 40 (1998), 263/280.
- [22] J. J. Harrigan, S. R. Reid and C. Peng: International Journal of Impact Engineering, 22 (1999), 955/979.
- [23] H. Yang and L. Zhaorong: Forming limits and die parameters of inverting-forming of thin-wall tubes, Proc 17th IDDRG, Shenyang, China, pp. 324-331, 1992.
- [24] H. Yang, S. Zhichao, J. Yingjun: Journal of Materials Processing Technology, 115 (2001), 367/372.
- [25] Z. Sun, H. Yang: International Journal of Machine Tools & Manufacture, 42 (2002), 15/20.
- [26] L. Schaeffer, A. M. G. Brito and M. Geier: Steel Research International, 76 (2005), 199/204.
- [27] A. N. Levanov: Journal of Materials Processing Technology, 72 (1997), 314/316.
- [28] T. Allan: Journal of Mechanical Engineering Science, 10 (1968), 182/197.